

# Modeling of Hot Carrier Degradation Using a Spherical Harmonics Expansion of the Bipolar Boltzmann Transport Equation

M. Bina<sup>◇,●</sup>, K. Rupp<sup>●,†</sup>, S. Tyaginov<sup>●</sup>, O. Triebel<sup>●</sup>, and T. Grasser<sup>●</sup>

<sup>◇</sup>Christian Doppler Laboratory for Reliability in Microelectronics at the <sup>●</sup>Institute for Microelectronics, TU Wien, Austria

<sup>†</sup>Institute for Analysis and Scientific Computing, TU Wien, Austria

## Abstract

Recent studies have clearly demonstrated that the degradation of MOS transistors due to hot carriers is highly sensitive to the energy distribution of the carriers. These distributions can only be obtained in sufficient detail by the simultaneous solution of the Boltzmann transport equation (BTE) for both carrier types. For predictive simulations, the energy distributions have to be thoroughly resolved by including the fullband structure, impact ionization (II), electron-electron scattering (EE), as well as the interaction of minority carriers with the majority carriers. We demonstrate that this challenging problem can be efficiently tackled using a deterministic approach based on the spherical harmonics expansion (SHE) of the BTE.

## Introduction

While the first hot-carrier degradation (HCD) models were based around the channel electric field as the driving force, it has long been realized that the phenomenon is energy-rather than field-driven [1]. In order to obtain the energy distribution, the BTE has to be solved, which is challenging in its own right. Unfortunately, as HCD is highly sensitive to the high-energy tail of the distribution, therefore the modeling of the scattering operator requires special attention. In particular, impact ionization scattering as well as electron-electron interactions have to be incorporated. For example, it has been shown that the adequacy of the BTE solution ignoring electron-electron scattering can be seriously hampered [2]. Furthermore, it has been shown that the majority carriers can significantly contribute to the damage, requiring a coupled solution of the BTE for electrons and holes [3]. Finally, since an accurate resolution of the energy distribution at high energies is required, information about the full band structure has to be included into the model. Traditionally, this complicated problem has been approached by using the Monte Carlo method (MC) [4], which is computationally- and time-intensive, particularly when the high-energy tails of the distribution function have to be resolved in detail [5]. In this work we demonstrate a time-efficient SHE solution of the bipolar BTE, which is applied to the investigation of HCD in n-channel MOSFETs.

## Method

We solve the Poisson equation and the bipolar BTE self-consistently on unstructured grids using the higher-order spherical harmonics expansion (SHE) simulator, ViennaSHE [6–8]. Full-band effects in silicon are accounted for using the method suggested by [9–11], cf. Fig 1.

The scattering mechanisms considered are acoustical and optical phonon scattering, impurity scattering, impact ionization (II) [4] with secondary carrier generation and electron

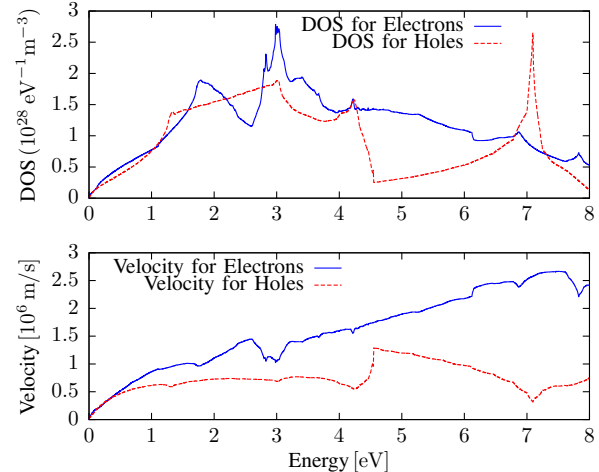


**Fig. 1:** The density of states (DOS) and group velocity for relaxed silicon used for the solution of the bipolar BTE with SHE expansion techniques. The DOS is efficiently incorporated into the SHE of the BTE using the approximation put forward by [9, 10].

electron scattering (EE) [12]. To assess the damage caused by hot carriers, the acceleration integral (AI) defined as

$$\sigma_0 \int f(\epsilon) Z(\epsilon) \left( \frac{\epsilon - E_{\text{th}}}{1 \text{ eV}} \right)^p v_g(\epsilon) d\epsilon, \quad (1)$$

has to be calculated, where  $\sigma_0$  is the capture cross section,  $p = 11$ ,  $f(\epsilon)$  is the distribution function,  $Z(\epsilon)$  the density of states (DOS),  $v_g(\epsilon)$  the group velocity and  $\epsilon$  is the carrier energy [13, 14]. The AI is the kernel of the hot carrier degradation model and is used to describe single- and multiple-carrier bond dissociation processes [3, 13, 15]. To simulate the device degradation, measured as a relative decrease in  $I_{d,\text{lin}}$ , we use the acceleration integrals for electrons and holes in our detailed degradation model [3]. Using this approach, two 2D n-channel MOSFETs with 250 nm and 25 nm channel lengths subjected to hot carrier stress at high oxide ( $\approx 8 \text{ MV/cm}$ ) and lateral electric fields ( $\approx 1 \text{ MV/cm}$ ) are investigated to assess the numerical and physical properties of the distribution function and acceleration integral. Interface states generated at the semiconductor-oxide interface during HCD disturb the electrostatics of the device and effect the carrier mobility. To incorporate these effects in a self-consistent manner, the AI was evaluated and used within our degradation model [3] to calculate the interface state density  $N_{\text{it}}$  at each simulation step. Additionally in every step the obtained  $N_{\text{it}}$  was used for the self-consistent treatment of trapped charges using Shockley-Read-Hall (SRH) theory [8]. These trapped charges act as coulomb scattering centers, thereby degrading the charge carrier mobility. Since it is not yet clear whether interface or oxide traps generated during HCD are governed by SRH trapping dynamics [16], the framework of ViennaSHE allows for the inclusion of arbitrary defect models.

## Results

To demonstrate the impact and the relative computational effort of the various degrees of sophistication, the ‘conventional’ BTE with impurity and phonon scattering only (cf. Fig. 2) was solved first and used as an initial guess for the subsequent simulations. Thus, the computational effort in terms of memory (cf. Fig. 6) and CPU-time (cf. Fig. 5) could be separated on the basis of the employed scattering mechanisms. As expected, if only basic scattering mechanisms

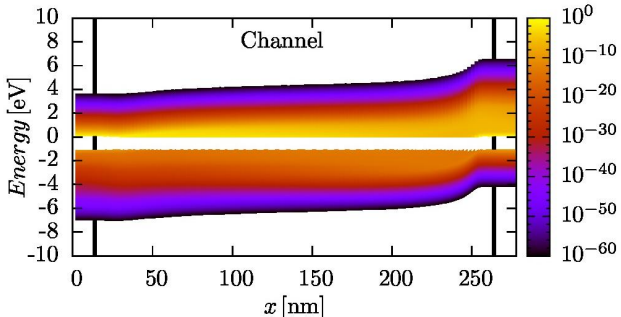


**Fig. 2:** The energy distribution function for high lateral field at the gate oxide interface for holes and electrons in a 250 nm n-channel MOSFET, where the source is located on the left hand side and the drain on the right hand side. In this case only phonon and impurity scattering mechanisms were considered and the distribution function decays rapidly with energy.

are used during the simulation, the probability for an electron or hole at the gate oxide interface to cause degradation is quite low (cf. Fig. 2). When EE scattering is additionally employed, the distribution function for electrons is elevated, while the distribution function for holes does not change significantly (cf. Fig. 3). When II scattering is also considered in addition, the probability of finding an electron or a hole at high energies is significantly higher compared to the cases without II (cf. Fig. 4). This is also reflected in the AIs for both the 250 nm and the 25 nm nMOSFET (cf. Figs. 9, 12). Electron electron scattering in the long channel device causes an almost uniform shift to higher values of the AI for electrons, but not for holes (cf. Fig. 9). This is directly reflected in the distribution functions (cf. Fig. 10) and the  $I_{d,\text{lin}}$  degradation (cf. Fig. 11). For the short channel device (25 nm) the shift caused by EE scattering is significantly higher close to the source as compared to the long channel MOSFET (cf. Fig. 12). The reinforcement of the  $I_{d,\text{lin}}$  degradation towards long stress

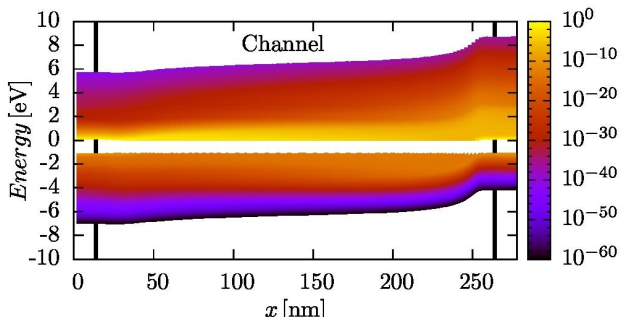


**Fig. 3:** Same as Fig. 2, but with EE scattering included. It can be seen that the EDF for electrons now decays much slower due to EE scattering compared to the EDF for electrons in Fig. 2. The EDF for holes is not impacted.

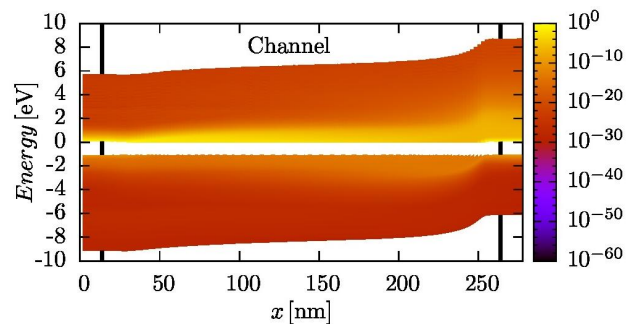


**Fig. 4:** Similar to Fig. 2 and Fig. 3, but with impact ionization considered. Now both electrons and holes gain higher carrier energies and the carrier temperatures are considerably elevated reaching the highest carrier energies under the spacer near the drain.

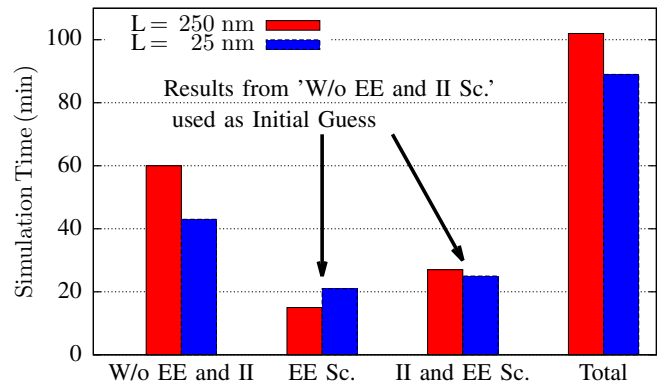


**Fig. 5:** The time needed to compute the distribution functions for each case and the total simulation time. It can be seen that the simulations in which EE and II scattering were not considered took longer to finish than for those additionally considering EE or EE and II scattering. All simulations have been performed on a machine equipped with an AMD Phenom II X6 1090 T processor using up to six cores.

times for electrons with II scattering in the 25 nm n-channel device is clearly visible in the  $I_{d,\text{lin}}$  degradation (cf. Fig. 14). II causes a dramatic increase in the AI for electrons in the long channel device (cf. Fig. 9) near the drain and a slight increase of the AI for holes near the source. It is interesting to note that in the short channel device II with EE scattering compared to the case without II causes no further increase in the AI for electrons close to the drain (cf. Fig. 12). This can be attributed to the electric field in short channel and a loss in carrier energy through EE scattering near the drain. Although II only causes a slight additional increase in the AI, it heavily increases the  $I_{d,\text{lin}}$  degradation over time. With all scattering mechanisms considered, one can clearly see the differences between short and long channel devices in the  $N_{it}$  profiles, caused by hot carriers (cf. Fig. 7 and Fig. 8). It is apparent that the minority carriers (holes) play a smaller role during HCD in the long channel device (cf. Fig. 7) as compared to the short channel device, where they massively contribute to the hot carrier induced damage (cf. Fig. 8) and cause a huge  $N_{it}$  increase over directly under the gate oxide.

## Conclusion

We have demonstrated the feasibility of the SHE method to efficiently solve the bipolar BTE including electron-electron, impact ionization scattering and semiconductor-oxide traps

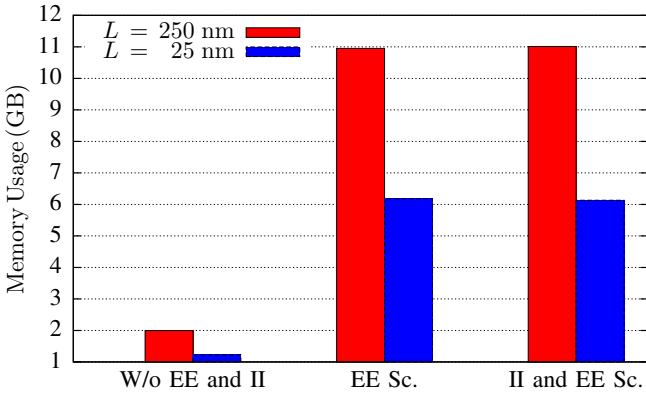


**Fig. 6:** The total random access memory used for each case. Whilst the simulations incorporating only phonon and impurity scattering took longer than the incremental others, they required considerably less memory (cf Fig. 5). The most memory was needed for the long channel device ( $L = 250 \text{ nm}$ ), since more meshpoints had to be used to achieve the same degree of spatial discretisation as for the short channel device ( $L = 25 \text{ nm}$ ). It can also be seen that using EE scattering results in a significantly higher memory consumption. This is due to the additional coupling introduced by the non-linear EE scattering operator.

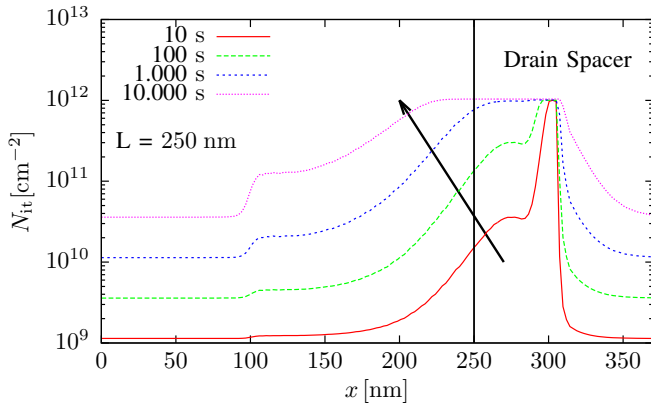


**Fig. 7:** The defect density  $N_{it}$  over gate length at the semiconductor-oxide interface after hot carrier stress for the  $250 \text{ nm}$  n-channel device.  $N_{it}$  under the gate increases with stress time as previously published [3].

self-consistently. As demonstrated, such a level of detail is required for the study of hot carrier degradation. However, it can be expected that many other hot carrier phenomena such as hot electron tunneling currents, memory cell programming and erase studies will benefit considerably from such a description as implemented in the free open-source simulator ViennaSHE.

### Acknowledgments

M. Bina, K. Rupp and T. Grasser acknowledge partial support by the Austrian Science Fund (FWF), grant P23598. S. Tyaginov thankfully acknowledges support by the Austrian Science Fund (FWF), grant P23958.

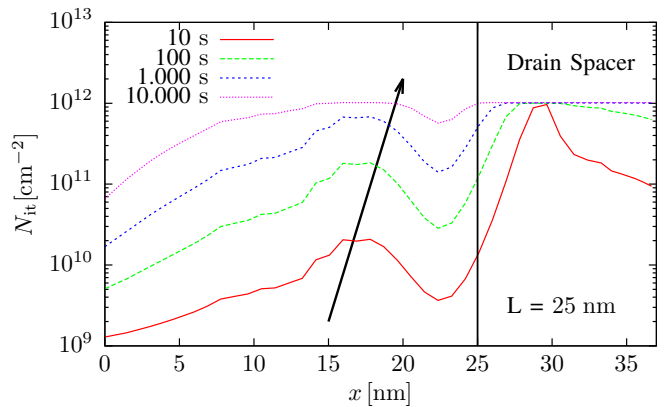


**Fig. 8:** The defect density  $N_{it}$  at the semiconductor-oxide interface over the gate length after hot carrier stress for the  $25 \text{ nm}$  channel device. Compared to the  $N_{it}$  profile (cf. Fig. 7) of the long channel device,  $N_{it}$  dominantly increases from the source side due to hole induced hot carrier damage.

### References

- [1] S. Rauch, F. Guarin, and G. La Rosa, "Impact of E-E scattering to the hot carrier degradation of deep submicron NMOSFETs," *IEEE Electron Device Letters*, vol. 19, no. 12, pp. 463–465, 1998.
- [2] A. Zaka, P. Palestri, Q. Rafhay, R. Clerc, M. Iellina, D. Rideau, C. Tavernier, G. Pananakakis, H. Jaouen, and L. Selmi, "An Efficient Nonlocal Hot Electron Model Accounting for Electron-Electron Scattering," *IEEE Transactions on Electron Devices*, vol. 59, no. 4, pp. 983–993, 2012.
- [3] S. Tyaginov, I. Starkov, O. Triebel, H. Enichlmair, C. Jungemann, J. Park, H. Ceric, and T. Grasser, "Secondary Generated Holes as a Crucial Component for Modeling of HC Degradation in High-voltage n-MOSFET," in *Proceedings of SISPAD*, pp. 123–126, 2011.
- [4] C. Jungemann and B. Meinerzhagen, *Hierarchical Device Simulation: The Monte-Carlo Perspective*, Springer, 2003.
- [5] B. Meinerzhagen, A. Pham, S.-M. Hong, and C. Jungemann, "Solving Boltzmann Transport Equation without Monte-Carlo Algorithms - New Methods for Industrial TCAD Applications," in *Proceedings of SISPAD*, pp. 293–296, 2010.
- [6] K. Rupp, T. Grasser, and A. Jungel, "On the Feasibility of Spherical Harmonics Expansions of the Boltzmann Transport Equation for Three-dimensional Device Geometries," in *2011 IEEE International Electron Devices Meeting (IEDM)*, pp. 34.1.1–34.1.4, 2011.
- [7] K. Rupp, T. Grasser, and A. Jungel, "Adaptive Variable-order Spherical Harmonics Expansion of the Boltzmann Transport Equation," in *Proceedings of SISPAD*, pp. 151–154, 2011.
- [8] K. Rupp, C. Jungemann, M. Bina, A. Jungel, and T. Grasser, "Bipolar Spherical Harmonics Expansions of the Boltzmann Transport Equation," in *Proceedings of SISPAD*, pp. 19–22, 2012.
- [9] S. Jin, S.-M. Hong, and C. Jungemann, "An Efficient Approach to Include Full-Band Effects in Deterministic Boltzmann Equation Solver Based on High-Order Spherical Harmonics Expansion," *IEEE Transactions on Electron Devices*, vol. 58, no. 5, pp. 1287–1294, 2011.
- [10] S. Hong, A. Pham, and C. Jungemann, *Deterministic Solvers for the Boltzmann Transport Equation*, Springer, 2011.
- [11] M. Vecchi and M. Rudan, "Modeling Electron and Hole Transport with Full-band Structure Effects by means of the Spherical-Harmonics Expansion of the BTE," *IEEE Transactions on Electron Devices*, vol. 45, no. 1, pp. 230–238, 1998.
- [12] K. Rupp, T. Grasser, and A. Jungel, "Inclusion of Carrier-Carrier-Scattering Into Arbitrary-Order Spherical Harmonics Expansions of the Boltzmann Transport Equation," in *IWCE*, pp. 34.1.1–34.1.4, 2012.
- [13] W. McMahon, A. Haggag, and K. Hess, "Reliability Scaling Issues for Nanoscale Devices," *IEEE Trans. Nanotech.*, vol. 2, no. 1, pp. 33–38, 2003.
- [14] S. Tyaginov, I. Starkov, H. Enichlmair, J. Park, C. Jungemann, and T. Grasser, "Physics-Based Hot-Carrier Degradation Models," *ECS Transactions*, 2011.
- [15] A. Bravaix and V. Huard, "Hot-Carrier Degradation Issues in Advanced CMOS Nodes," in *European Symposium on the Reliability of Electron Devices*, 2010.
- [16] T. Grasser, "Stochastic Charge Trapping in Oxides: From Random Telegraph Noise to Bias Temperature Instabilities," *Microelectronics Reliability*, vol. 52, no. 1, pp. 39–70, 2012.

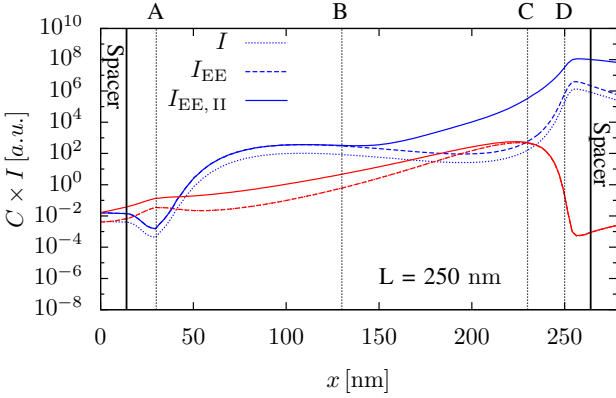


**Fig. 9:** The acceleration integrals along the gate oxide interface from the source to drain, computed from a bipolar solution of the BTE comparing phonon and impurity scattering, II scattering and EE scattering in a 250 nm n-channel device under hot carrier stress. In Fig. 10 the energy distribution functions used to compute the acceleration integrals at the points A, B, C and D are plotted. Note that points C and D correspond to the maxima of electron and hole AIIs, respectively.

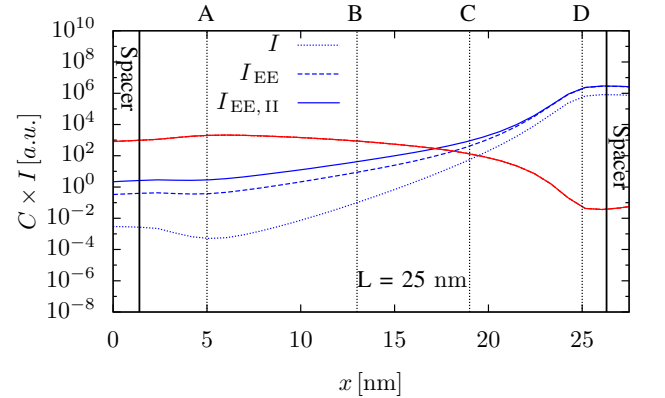


**Fig. 12:** The acceleration integrals along the gate oxide interface from the source to drain. The influence of EE scattering on the AI as compared to the AIs for the long channel device (cf. Fig. 9) is much more significant, whilst the influence of II is small. The AI for holes directly under the gate is higher in magnitude, when compared to the long channel device (cf. Fig. 9) which will cause a significant increase in  $N_{it}$  over time directly under the gate (cf. Fig. 8).

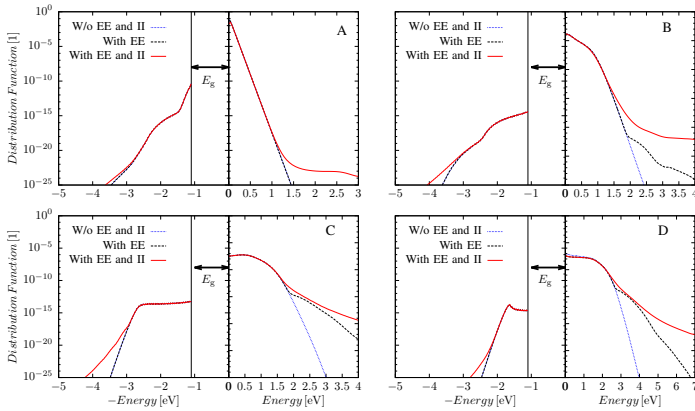


**Fig. 10:** The energy distribution functions for electrons and holes used to compute the acceleration integrals at the points A, B, C and D in Fig. 9 for the long channel device.

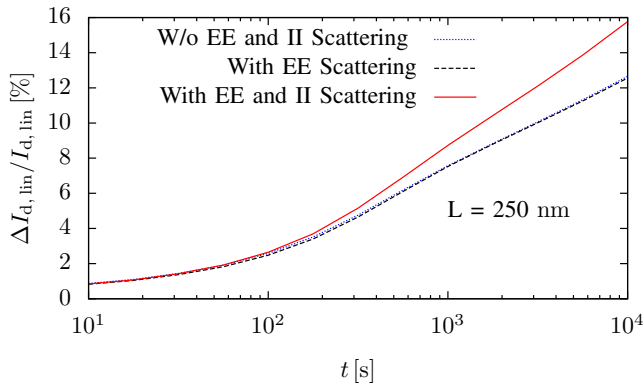


**Fig. 11:** Relative  $\Delta I_{d,lin}$  for the long channel device under hot carrier stress over the stress time. The  $I_{d,lin}$  change was calculated using our hot carrier degradation model. In the long channel device under stress EE scattering has only a small influence, whilst the influence of impact ionization is large towards long stress durations. The main effect of EE scattering is that it lowers the degradation for short stress times and elevates  $\Delta I_{d,lin}$  for longer periods of hot carrier stress.

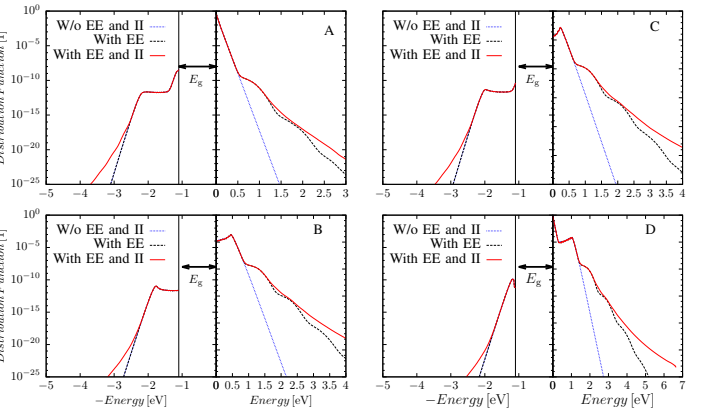


**Fig. 13:** The energy distribution functions for electrons and holes at the points A, B, C and D in Fig. 12 used to compute the acceleration integrals.

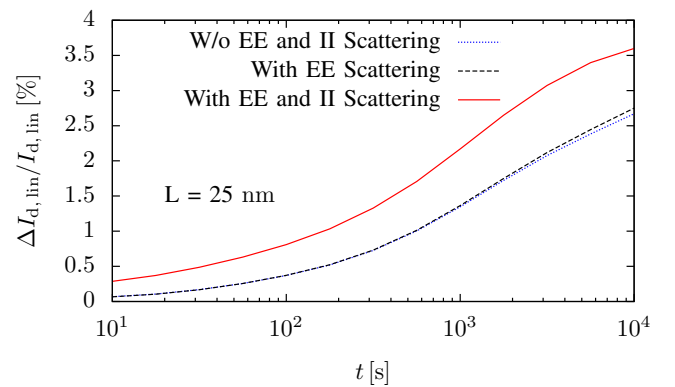


**Fig. 14:** Similar to Fig. 11, but for the short channel (25 nm) device. EE scattering has the same qualitative, though stronger effect in magnitude in short channel MOSFETs as compared to their long channel counterparts (cf. Fig. 11). II in short channel transistors considerably elevates the relative  $\Delta I_{d,lin}$  change over the whole range of stress times, getting more significant for longer periods of stress.